CENTRE NATIONAL DE LA RECHERCHE SCIENTIFIQUE

LABORATOIRE D'ANALYSE ET D'ARCHITECTURE DES SYSTEMES

STUDY OF AN INTEGRATED ELECTRONIC MONITOR FOR NEUTRON BEAMS

B. BARELAUD, F. NEXON-MOKHTARI, C. BARRAU, J.L. DECOSSAS, J.C.VAREILLE, G. SARRABAYROUSE

CNRS -

LAAS REPORT 94428

OCTOBER 1994

STUDY OF AN INTEGRATED ELECTRONIC MONITOR FOR NEUTRON BEAMS

B. BARELAUD, F. NEXON-MOKHTARI, C. BARRAU, J.L. DECOSSAS, J.C. VAREILLE

LEPOFI, University of Limoges, 123, avenue Albert Thomas

87060 LIMOGES CEDEX - FRANCE

G. SARRABAYROUSE

LAAS, CNRS, 7, avenue du Colonel Roche

31400 TOULOUSE - FRANCE

Abstract : The majority of the individual neutron monitorings presents an energy range (10 keV - 500 keV) where the measure is uncorrect. For electronic devices, this problem is due to their high γ sensitivity.

In order to solve this problem, a microelectronic structure design for neutron spectrometry is now being studied at LEPOFI. Basically it consists in analysing the total energy which is deposited by ^{6}Li (n, α) ^{3}H or ^{10}B (n, α) ^{7}Li reactions in silicon detectors.

A new electronic sensor - for example a boron or lithium sandwich device (1) - has been realized in collaboration with LAAS. Specific techniques for silicon sensors coating with boron have been developped and are briefly presented.

The response has been computed thanks to a model and a code developped at LEPOFI. Several parameters have been taken into account in the calculations : the nature of layer, its thickness, the characteristics of detectors. The energy distribution of pulses has been calculated.

INTRODUCTION

Fast neutron dosimetry is generally based on the detection of recoil protons from an hydrogenous converter which can be specific or part of the detector itself (solid state nuclear track detectors) [2]. A few tenth of micrometers thickness leads to a response (tracks or pulses per square centimeter per millisievert) almost independent of neutron energy [3]. Additionnally, thermal neutron dosimetry can be realized by adding ^{10}B or ^{6}Li on the converter. Nevertheless the whole energy range is not correctly covered, particularly the 10 keV - 500 keV domain.

For this range, the development of research on active neutron dosimetry has shown that the main drawback of electronic devices is their γ sensitivity [4] (figure 1). In terms of dose equivalent the gamma component of mixed fields of interest is almost equal to the neutron one, whereas a cutoff at 150 keV, for the same dose equivalent, the number of gamma pulses delivered by a diode can be 400 times greater than the number of neutron pulses [5]. The differential measurements proposed by our laboratory [6, 7] improve the neutron pulses discrimination, thus reduce the neutron energy threshold, but become inoperative when the gamma component is too important.

In order to solve this problem, several methods have been proposed or are in progress in the frame of a CEC contract :

- an increase of the neutron signal thanks to a slowing down of neutrons combined with their detection through a nuclear reaction [8] ;

- a decrease of the γ pulses by removing all high Z parts of the sensor which produce most of the Compton electrons ;

- the analysis and discrimination of the rise times of the neutron and gamma pulses [9].

A reduced size of the detecting volume (depleted zone in an integrated transistor) has also been studied through the use of SRAM [10, 11].

An alternative is now being studied at LEPOFI University of LIMOGES - FRANCE in collaboration with LAAS CNRS TOULOUSE - FRANCE, with the aim is to characterize the neutron field. The studied device works as a spectrometer based on ^{10}B (n, α) ^{7}Li or ^{6}Li (n, α) ^{3}H reactions. The reaction products are detected in coïncidence. This coïncidence detection is combined with an electronic threshold to eliminate the gamma background of realistic fields. It is now too early to foresee the possibilities of this device and the present paper intends to present the first studies of the sensor. Two basic questions, which imply many others, are : is it possible to study then develop the device as a spectrometer, a dosemeter or both ? Will microelectronic technology be able to realize the sensor and, if a individual monitoring is wished, to integrate all the functions necessary for signal analysis ?

The results and analyses proposed in this paper concern a preliminary study which wishes to show that the device is feasible and could work properly. This first step includes the modeling of the device and Monte-Carlo calculations of the properties, as well as the realization of a basic first prototype.

PRINCIPLE

The sensor

A diagram of the sensor is given on figure 2. It is composed of two facing diodes between which is a layer of boron 10 or lithium 6. These two elements are well adapted to microelectronic technologies. For this first approach, the use of boron (coating, etching...) being more mastered than that of lithium, ^{10}B was chosen for the realization of the first prototype. Nevertheless the results of calculations that are presented concern lithium as well as boron.

The parameters influencing the response of the structure proposed in figure 2 are the following :

- the amount of reactive product which defines the sensitivity of the sensor. The area of the boron or lithium layer is limited by the area of usual wafers available for microelectronic chips. It is obvious that an increasing of layer thickness produces an absorption of the particles from nuclear reactions that occur inside the layer. One can easily foresee that spectrometric properties need a layer as thin as possible not compatible with the need of high sensitivity necessary for dosimetry.

- the thickness of the dead layer of the detecting diodes. It must be minimized since it always acts as an absorber of the energy of the recoils, and it is obvious that these particles, if they have a very oblique trajectory, loose an important part of their energy, or even can be absorbed.

- the thickness of the depleted layer must be adapted to the range of the most energetic particles crossing normaly the various layers. For calculations this condition is supposed to be realized.

- the bulk of the wafer is supposed not to have any influence on the response of the sensor.

Detection electronics

It is an usual coïncidence system (figure 3). Several possibilities have been prepared for experiments which allow to measure the spectra on each detector or, by summing the pulses from both detectors, to get the distribution of the total energy of the nuclear reaction particles.

MODELING THE RESPONSE

The sensor response has been modeled thanks to Monte-Carlo calculation codes developped in our laboratory. ENDF B VI library taken from NEA has been used for neutron data. The stopping power for secondary particles in the different materials of the sensor have been calculated using TRIM-91 program.

The response must be calculated for monoenergetic neutrons (from thermal up to several MeV) as well as for spectra. For thermal neutrons the problem is rather simple, the reaction being isotropic. The results are available and are presented.

For fast neutrons the isotropy of the reaction is no longer realized and the corresponding laws must be used. The response in spectra (sources, realistic fields) can be calculated using the same method. The modeling of the experimental pulse spectra needs to take into account the response of the electronic measuring device. All these points are now being studied.

The influence of albedo spectra when a phantom is used cannot be calculated for the moment as, as far as we know, these spectra have never been calculated or at least, not published.

So, the results we are now going to analyze concern thermal neutrons, and the spectra are the distributions of the energy which is deposited in depleted layers even if the term "pulse" spectrum is sometimes used. The resolution has not been taken into account and the widening of the peaks does not appear. We shall examine in turn the role of the parameters previously introduced : the dead layer, the reactive layer.

The dead layer

The assumptions that are necessary to show the role of the dead layer are simple : boron or lithium atoms on which the nuclear reactions occur are concentrated in an infinitely thin layer on the common surface of the two facing diodes. The reaction being isotropic, an emission angle is chosen at random. The particles are followed and the energy which is lost in the dead layer deduced from the initial energy. The distribution of the remaining energy is calculated. 10 keV energy steps have been used, and 10, 50, 100, 200, 500 nm thick dead zones have been considered, the thickness for usual diodes lying in this range. 10^5 interactions have been simulated. Sometimes this leads to visible statistical fluctuations but does not disturb the analysis, interpretation and understanding of the phenomena. Only few results among the great number of spectra calculated are presented.

Figures 4 and 5 show results concerning ^{10}B. The 3 first (4-a, b, c) are spectra detected by one of the diodes for 10, 100 and 500 nm thick dead layers. 100 and 500 nm results have been zoomed to underscore the modifications of the spectra by an increasing thickness of dead zone. Peaks of the two particles ^4_2He and ^7_3Li of fundamental and excited states of the reaction appear clearly. As the thickness increases two effects can be noted. Low energy pulses appear due to particles having had a long path in the dead layer. The maximum energy of the peak is also modified : for the ^7Li from the excited state, and 10 nm dead layer thickness, this maximum energy stays close to the basic 840 keV but decreases to 790 keV for 100 nm and falls down to 590 keV for 500 nm. The differences between these energies and the initial energy of the lithium correspond to the loss when the particle crosses perpendicularly the layer . Whatever the thickness, for the 1010 keV peak of the ^7Li from the fundamental state, the loss is similar (1010 keV $\rightarrow$ 750 keV at 500 nm) due to a similar LET in this energy range.

The distribution of the total energy deposited in coïncidence by one nuclear reaction has also been calculated for all the thicknesses already mentionned. An example is given in figure 5. The two possible values (Q = 2.31 MeV and Q = 2.79 MeV) appear and the zoomed part of the spectrum shows the details. In order to quantify the spectrum modification we have calculated the number of pulses having an energy lower than 0.95 E_{max} where E_{max} is the maximum energy of the peak ; results are given in table 1.

Figures 6 to 7 show the results for a ^6Li reactive layer. As for ^{10}B the 3 first illustrate the role of the dead layer thickness on the two peaks (the reaction has no excited state) detected by one of the diodes. The comments on ^{10}B results remain valid for ^6Li, but spectra are less disturbed.

The differences in the modifications can obviously be explained by the nature and energy of the particles : being lighter and more energetic than the ^{7}Li recoil, the ^{3}H has a lower LET. The comparison of the energy of the α particles of the two reactions leads to the same conclusion.

The reactive layer

Its thickness effect appears on figures 8 and 9 for ^{10}B and 10 and 11 for ^{6}Li. The corresponding calculations have, at the same time, taken into account the roles of the dead zone and of the reactive layer. They lead to the spectra of the deposited energy as it occurs in the structure of figure 2. The flattening of the peaks is explained by nuclear reactions occuring at random inside the reactive layer. This could be divided into elementary layers, each of them producing a contribution to the final spectrum. The sum of these elementary spectra wich are shifted from each other consists in a flattened final distribution. Figure 9 gives the spectrum of the total energy deposited in coïncidence for 100 nm of ^{10}B in 100 nm dead zone diodes. The same conditions for ^{6}Li give the results plotted on figure 11. For the reasons previously presented, the spectra are less disturbed in the second case.

The global analysis of the results shows that the thicknesses of the reactive layer and of the dead layer give the spectrometric properties of the device ; in these conditions the device must be realized with diodes having an as thin as possible dead layer. For neutron dosimetry the condition of a thin reactive layer could lead to a too low sensitivity. More complete studies including fast neutron response calculations are in progress. They will indicate if spectrometry and dosimetry with such a device are compatible aims. Nevertheless, in spite of the lack of calculated results for high energies the realization of a prototype of the sensor has been undertaken. As indicated, the boron technology has appeared to the more simple and suitable to develop a prototype for feasibility studies as described now.

REALIZATION OF THE SENSOR

The detector currently under investigation is schematized on figure 2. It is made of two ion implanted P^+-N diodes which are identical but one of them has received a ^{10}B deposition over the central region. Critical points in the fabrication process are the junction depths in the active area, Boron deposition and etching and finally the diodes alignement. In order to ensure a dead layer as thin as possible the P^+ regions outside the metal-semiconductor contact are obtained by a BF_2 implantation at low energy. The Boron etching is done by Reactive Ion Etching and the etching rate and the selectivity with respect to SiO_2 have been found satisfactory. Finally the alignement of the diodes is made by Infrared Radiography. The area of the active region is 2.25 cm^2.

CONCLUSION

In order to check our calculations and verify the properties theoretically established, several sensors having different thicknesses of reactive layer are now being realized. As previously outlined one of the major question about this device is its sensitivity. As an albedo dosemeter this sensitivity could be great enough since for a 100 nm thick ^{10}B layer, it is $4.5 \cdot 10^5$ pulses /mSv for a 1 cm^2 sensor. For fast neutrons, a first approximation can be calculated through cross sections of ^{10}B, but without taking into account important problems such as fast neutron pulses discrimination, non isotropic reaction... The sensitivity which was calculated for 1cm^2 of sensor is about 400 pulses /mSv at 15 keV and respectively 63 and 27 pulses /mSv at 50 and 100 keV.

ACKNOWLEDGEMENTS

Results presented in this paper were obtained in the frame of the CEC contract FI3P CT93 0072.

REFERENCES

(1) - KNOLL, G.F. Radiation Detection and Measurement - John Wiley & Sons, Inc. (U.S.A.) ISBN 0-471-49545-X (1979).

(2) - DECOSSAS, J.L., VAREILLE, J.C., MOLITON, J.P. and TEYSSIER, J.L. Theoretical study and calculation of the response of a fast neutron dosemeter based on track detection - Radiat. Prot. Dosim. **5** (3), 163-170 (1983).

(3) - SADAKA, S., MAKOVICKA, L., VAREILLE, J.C., DECOSSAS, J.L. and TEYSSIER , J.L. - Study of polyethylene and CR 39 fast neutron dosemeter II : Dosimetric efficiency of the device - Radiat. Prot. Dosim. **16** (4), 281-287 (1986).

(4) - PAUL, D., BARELAUD, B., DUBARRY, B., MAKOVICKA, L., VAREILLE , J.C. and DECOSSAS, J.L. - Gamma Interference on an electronic dosemeter response in a neutron field - Radiat. Prot. Dosim. **45** (1-4), 371-374 (1992).

(5) - BARELAUD, B., DUBARRY-CHABANAIS B., PAUL, D., MAKOVICKA, L., DECOSSAS, J.L. and VAREILLE, J.C. - Evolution du capteur électronique pour la dosimétrie des neutrons développé au LEPOFI - Radioprotection **28** (4), 387-409 (1993).

(6) - MAKOVICKA, L., DECOSSAS, J.L. and VAREILLE, J.C. - Experimental study of the dosimetric efficiency of a radiator - CR 39 fast neutron dosemeter - Radiat. Prot. Dosim. **20** (1-2), 63-67 (1987).

(7) - BARELAUD, B., PAUL, D., DUBARRY, B., MAKOVICKA, L., DECOSSAS, J.L. and VAREILLE, J.C. - Principles of an electronic neutron dosemeter using a PIPS detector - Radiat. Prot. Dosim. **44** (1-4) 363-366 (1992).

(8) - SAVVIDIS, E., SAMPSONIDIS, D. and ZAMANI, M. - A CR 39 fast neutron dosemeter based on (n, α) converter - Radiat. Prot. Dosim. **44** (1-4), 341-342 (1992).

(9) - BARTHE, J., LAHAYE, T. and BORDY, J.M. - Sensors for personal neutron dosemeters, Neutron Individual Dosimetry, EURADOS, NRPB (1994).

(10) - SCHRODER, T., SCHMITZ, T. and PIERSCHEL, M. - Microdosimetric dosemeters for individual monitoring based on semiconductor detectors - Radiat. Prot. Dosim. **52** (1-4), 431-434 (1994).

(11) - SCHRODER, T. and SCHMITZ, T. - Can a personal dosemeter for neutron radiation based on semiconductor chip match the new ICRP recommandations - Radiat. Prot. Dosim. **54** (3-4), 431-434 (1994).

Figure 1 : γ response of one diode.

Figure 2 : Schematized view of the detector.

Figure 3 : Schematic diagram of electronic neutron dosemeter.

Figure 4 : Spectrum from one diode with a boron 10 reactive layer :

a - dead zone thickness : 10 nm

b - dead zone thickness : 100 nm + zoom

c - dead zone thickness : 500 nm + zoom.

Figure 5 : Distribution of the total energy deposited in the sensor for 100 nm dead zone thickness and a boron 10 reactive layer.

Figure 6 : Spectrum from one diode with a lithium 6 reactive layer :

a - dead zone thickness : 10 nm

b - dead zone thickness : 100 nm + zoom

c - dead zone thickness : 500 nm + zoom.

Figure 7 : Distribution of the total energy deposited in the sensor for 100 nm dead zone thickness and a lithium 6 reactive layer.

Figure 8 : Spectrum from one diode for a 100 nm dead zone thickness :

a - Boron thickness : 100 nm

b - Boron thickness : 500 nm.

Figure 9 : Distribution of the total energy deposited in the sensor for 100 nm dead zone thickness and 100 nm boron thickness.

Figure 10 : Spectrum from one diode for a 100 nm dead zone thickness :

a - Lithium thickness : 100 nm

b - Lithium thickness : 500 nm.

Figure 11 : Distribution of the total energy deposited in the sensor for 100 nm dead zone thickness and 100 nm lithium thickness.

Table 1 : Ratio of the number of pulses between 0 and $0.9 \cdot E_{max}$ (or $0.95 \cdot E_{max}$) to the total number of pulses.

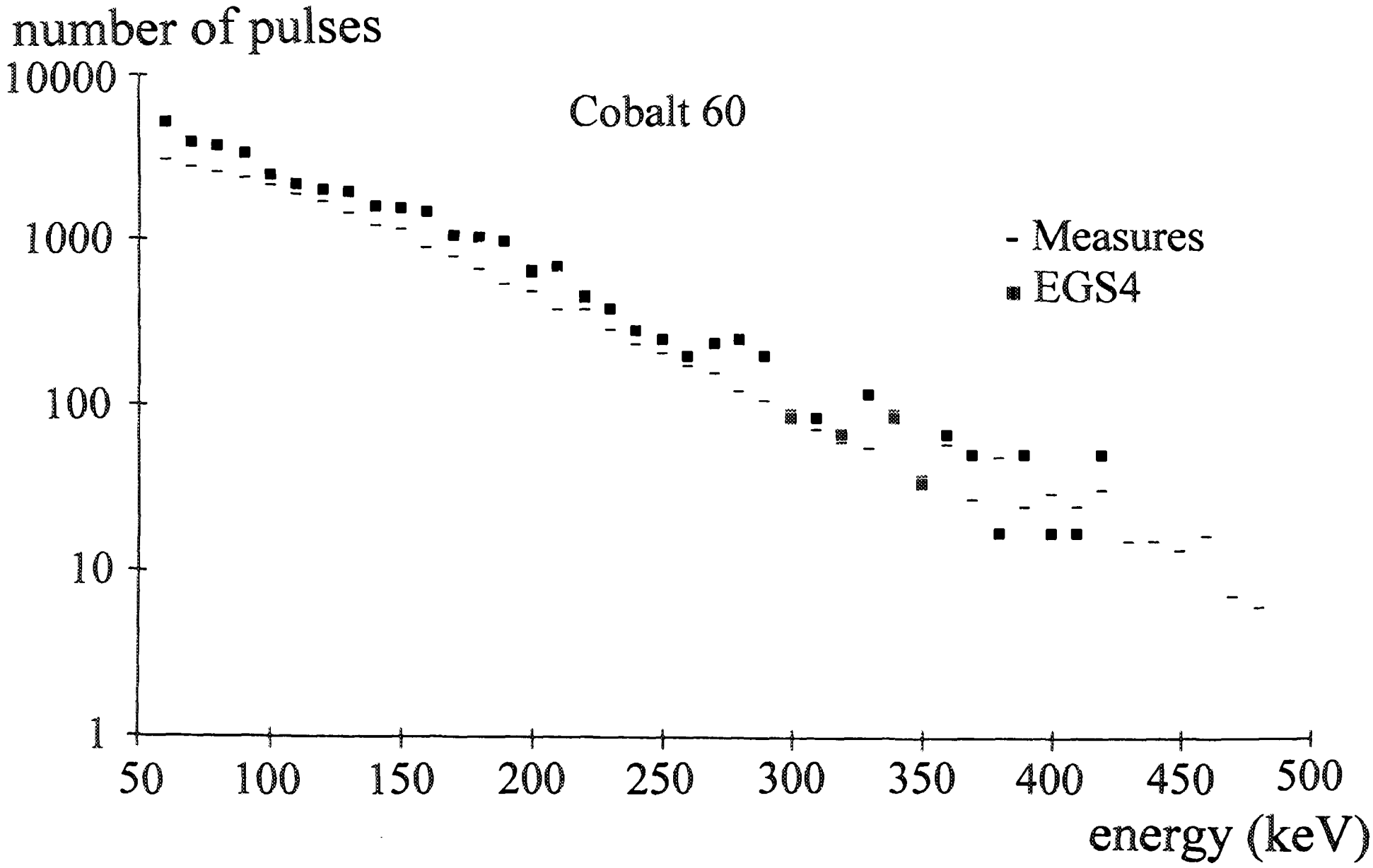
number of pulses
10000
1000
100
10
1
Cobalt 60
- Measures
EGS4
50
100
150
200
250
300
350
400
450
500
energy (keV)

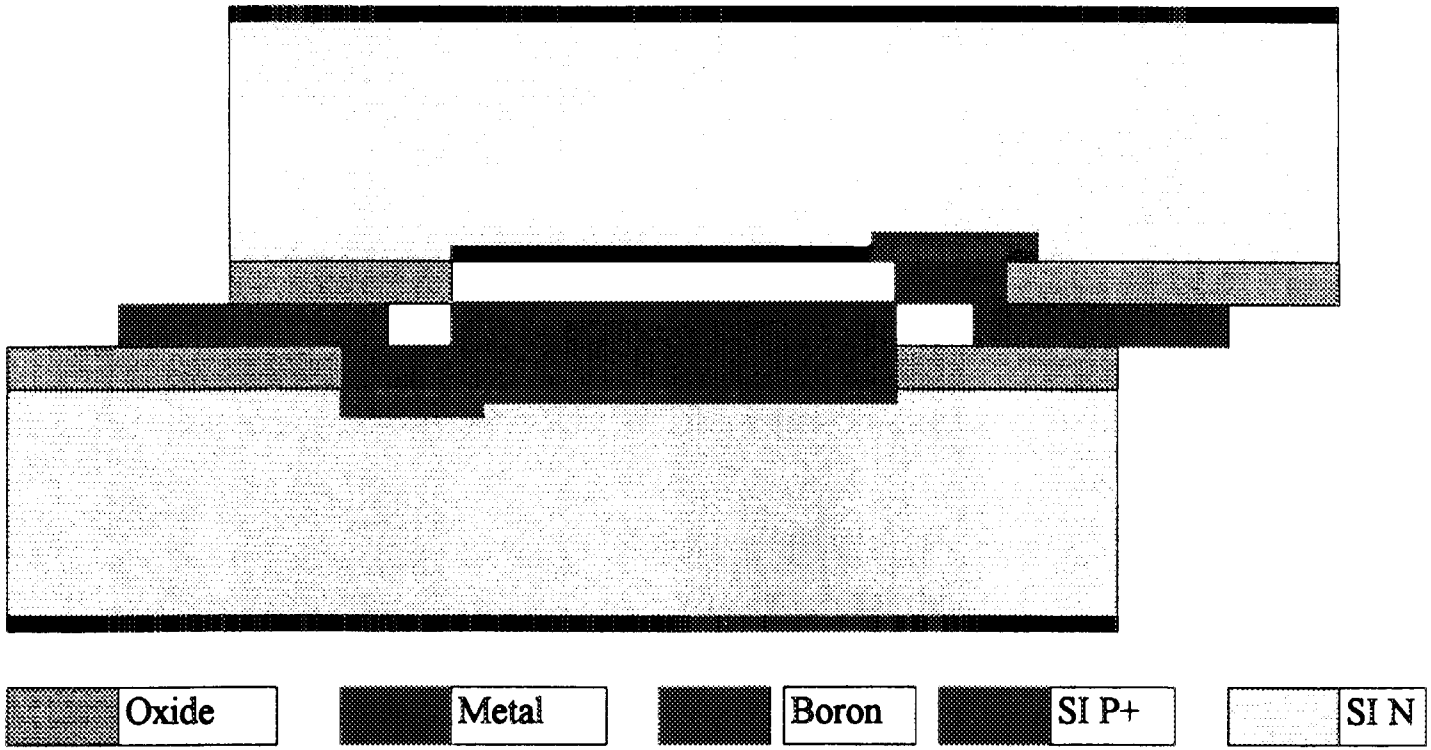
Oxide
Metal
Boron
SI P+
SI N

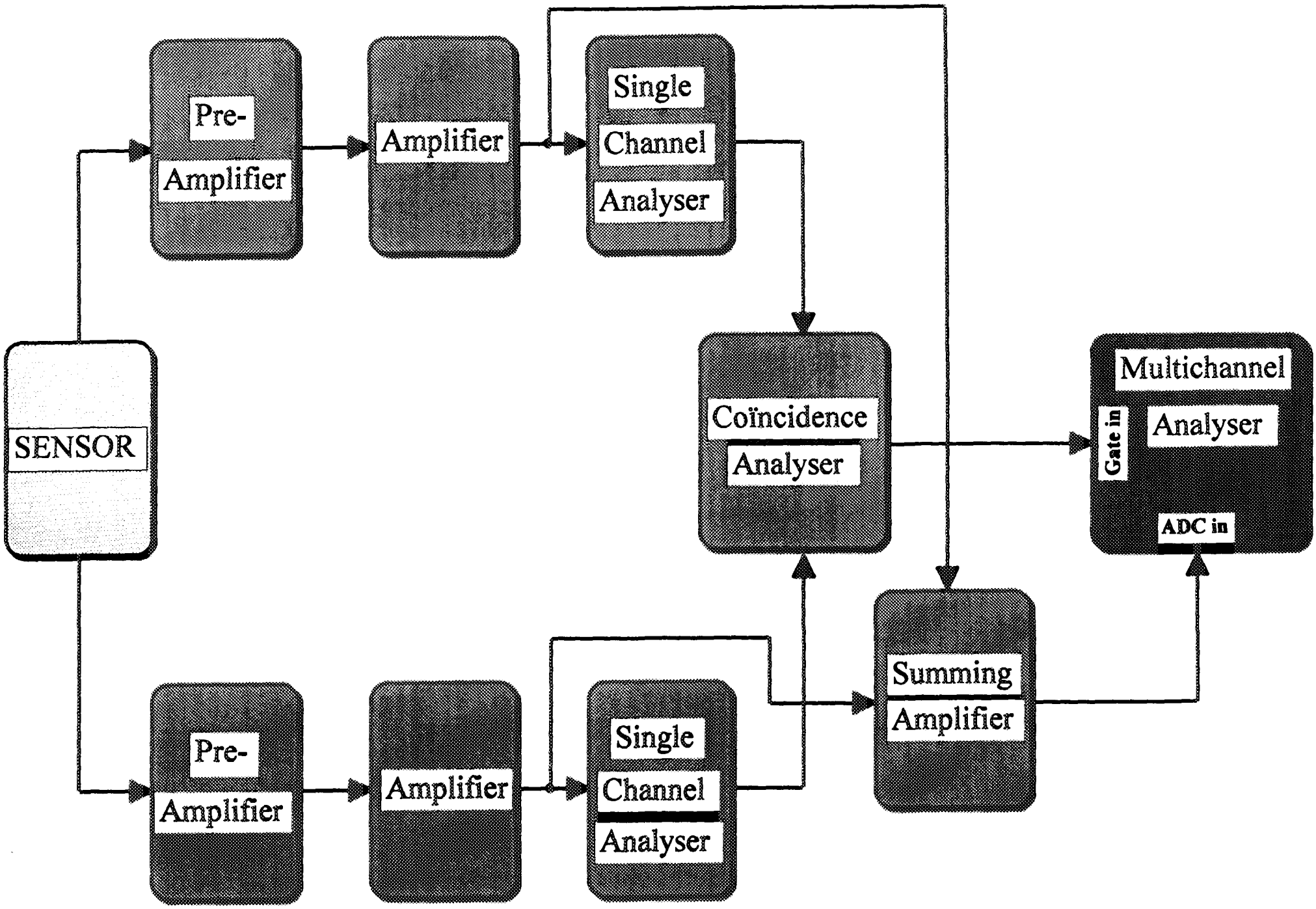
Pre-
Amplifier
Amplifier
Single
Channel
Analyser
SENSOR
Coïncidence
Analyser
Multichannel
Analyser
Gate in
ADC in
Summing
Amplifier
Pre-
Amplifier
Amplifier
Single
Channel
Analyser

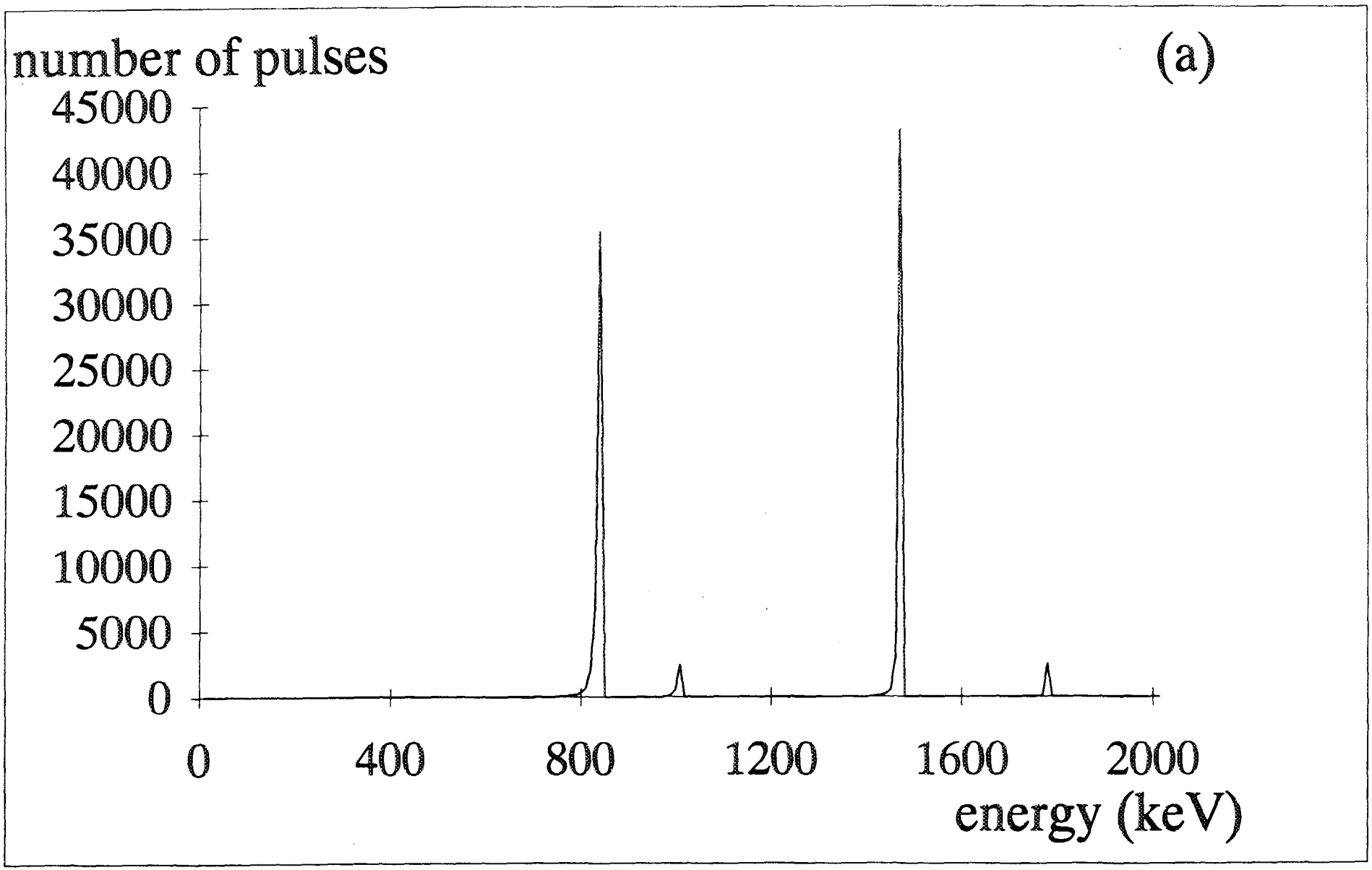
number of pulses
(a)
45000
40000
35000
30000
25000
20000
15000
10000
5000
0
0
400
800
1200
1600
2000
energy (keV)

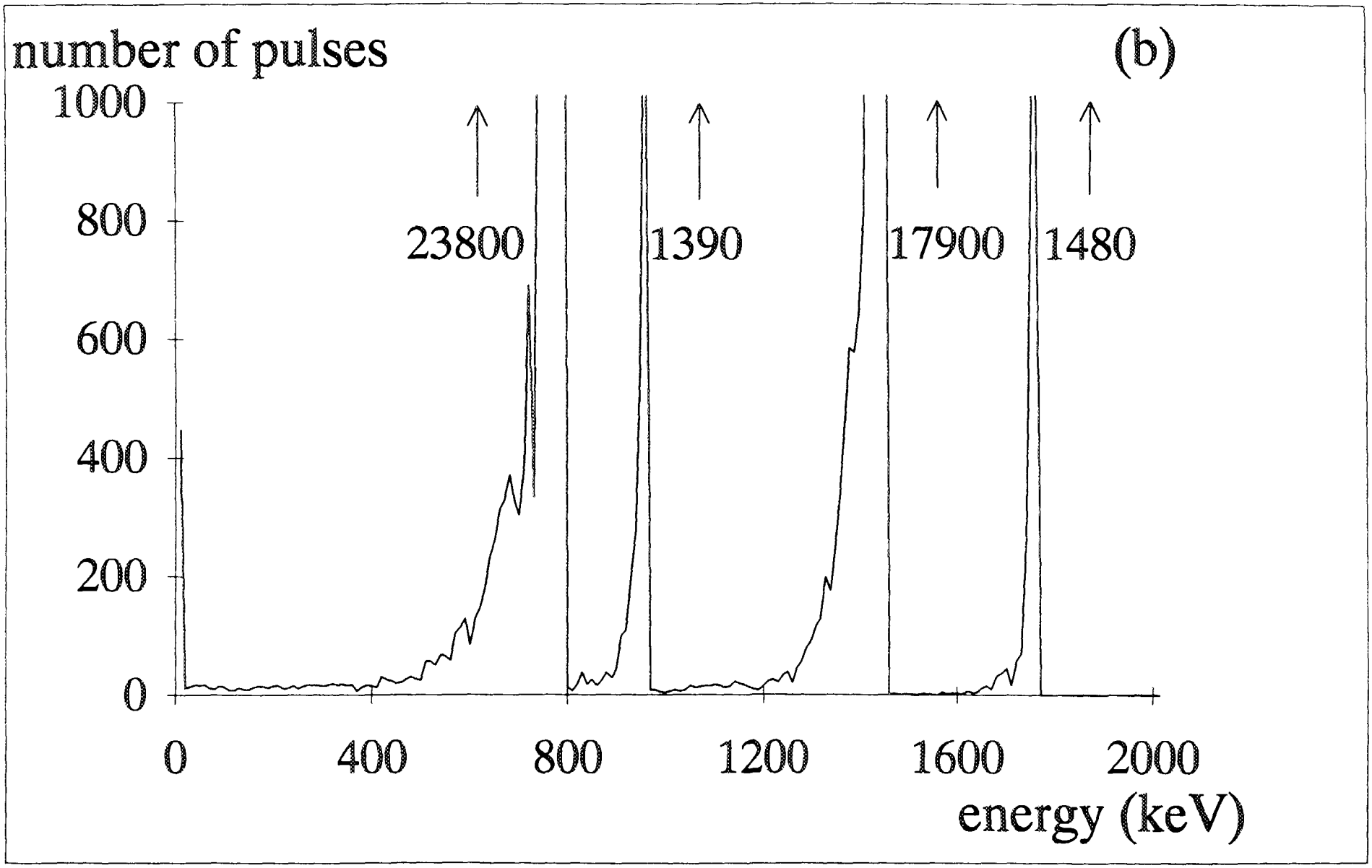
number of pulses
(b)
1000
800
600
400
200
0
23800
1390
17900
1480
0
400
800
1200
1600
2000
energy (keV)

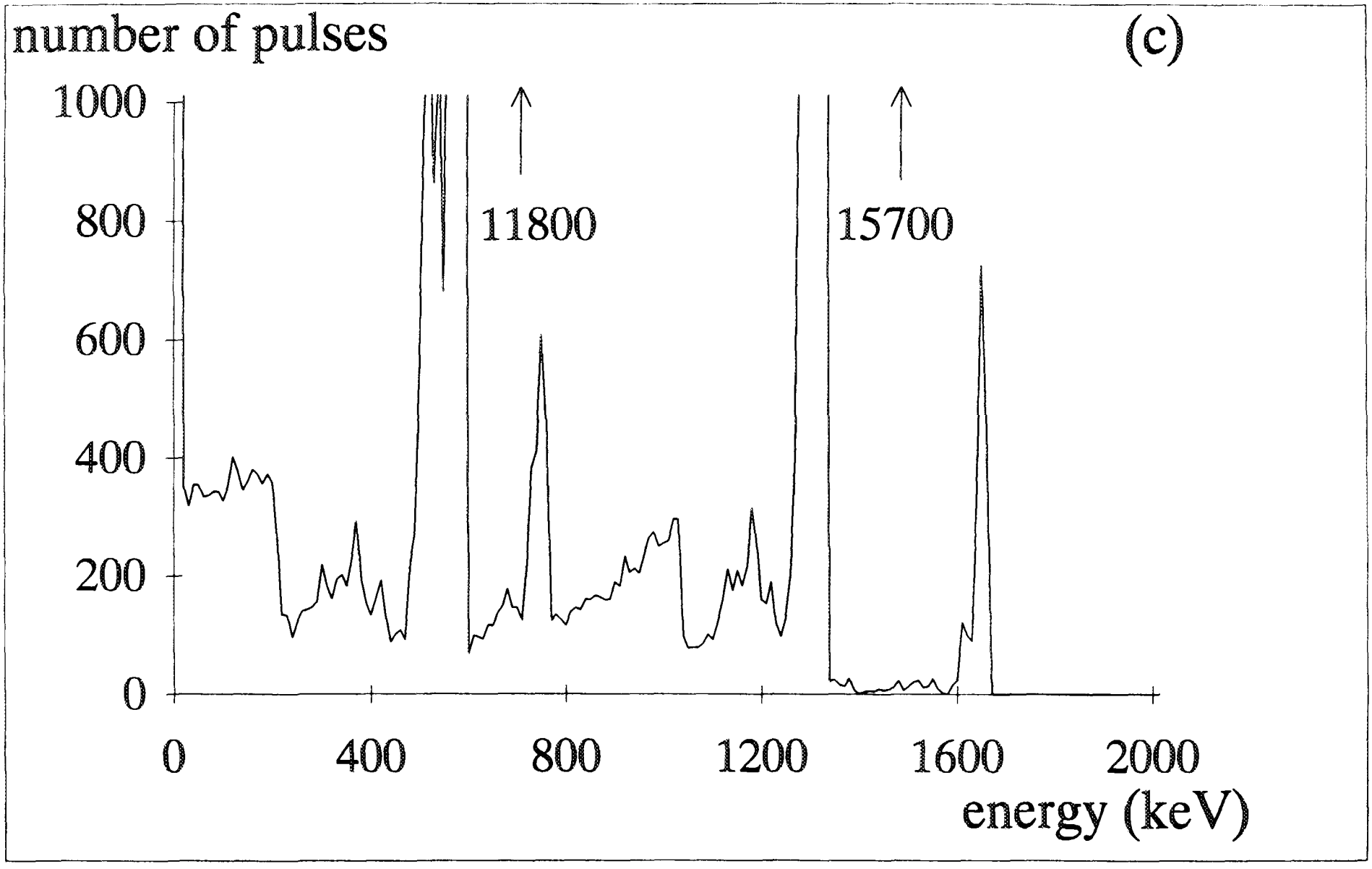
number of pulses
(c)
1000
800
600
400
200
0
11800
15700
0
400
800
1200
1600
2000
energy (keV)

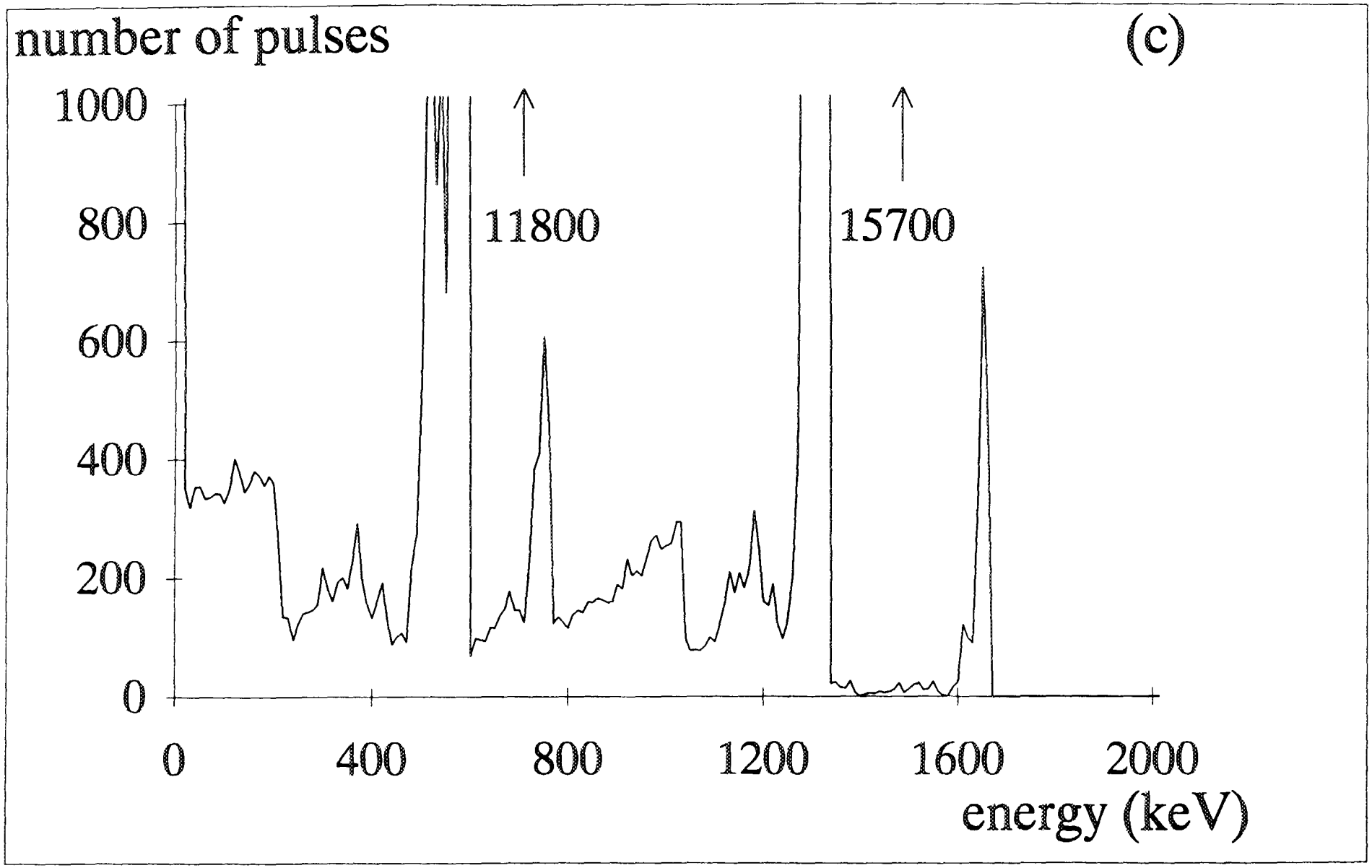
number of pulses
(c)
1000
800
600
400
200
0
11800
15700
0
400
800
1200
1600
2000
energy (keV)

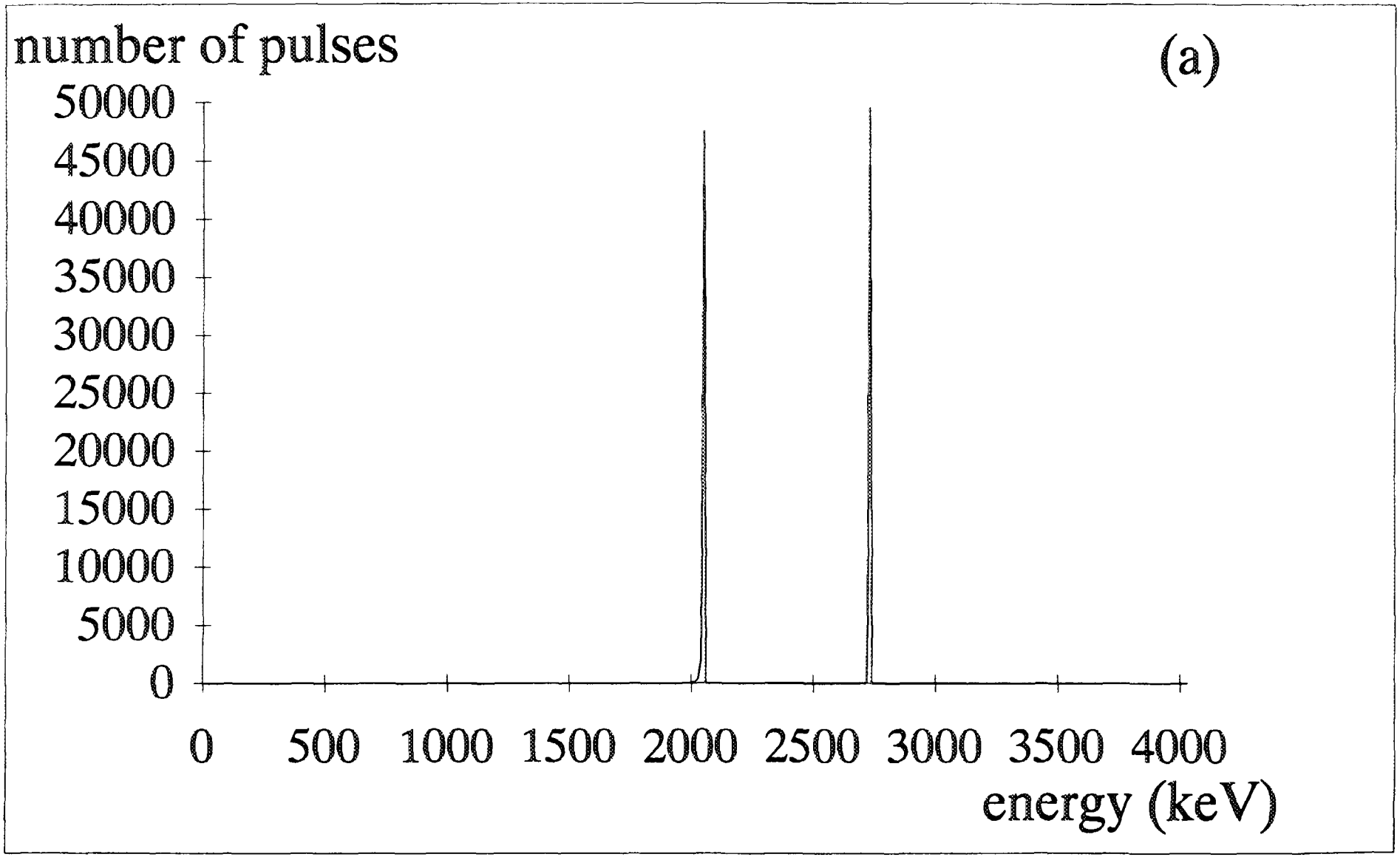
number of pulses
(a)
50000
45000
40000
35000
30000
25000
20000
15000
10000
5000
0
0
500
1000
1500
2000
2500
3000
3500
4000
energy (keV)

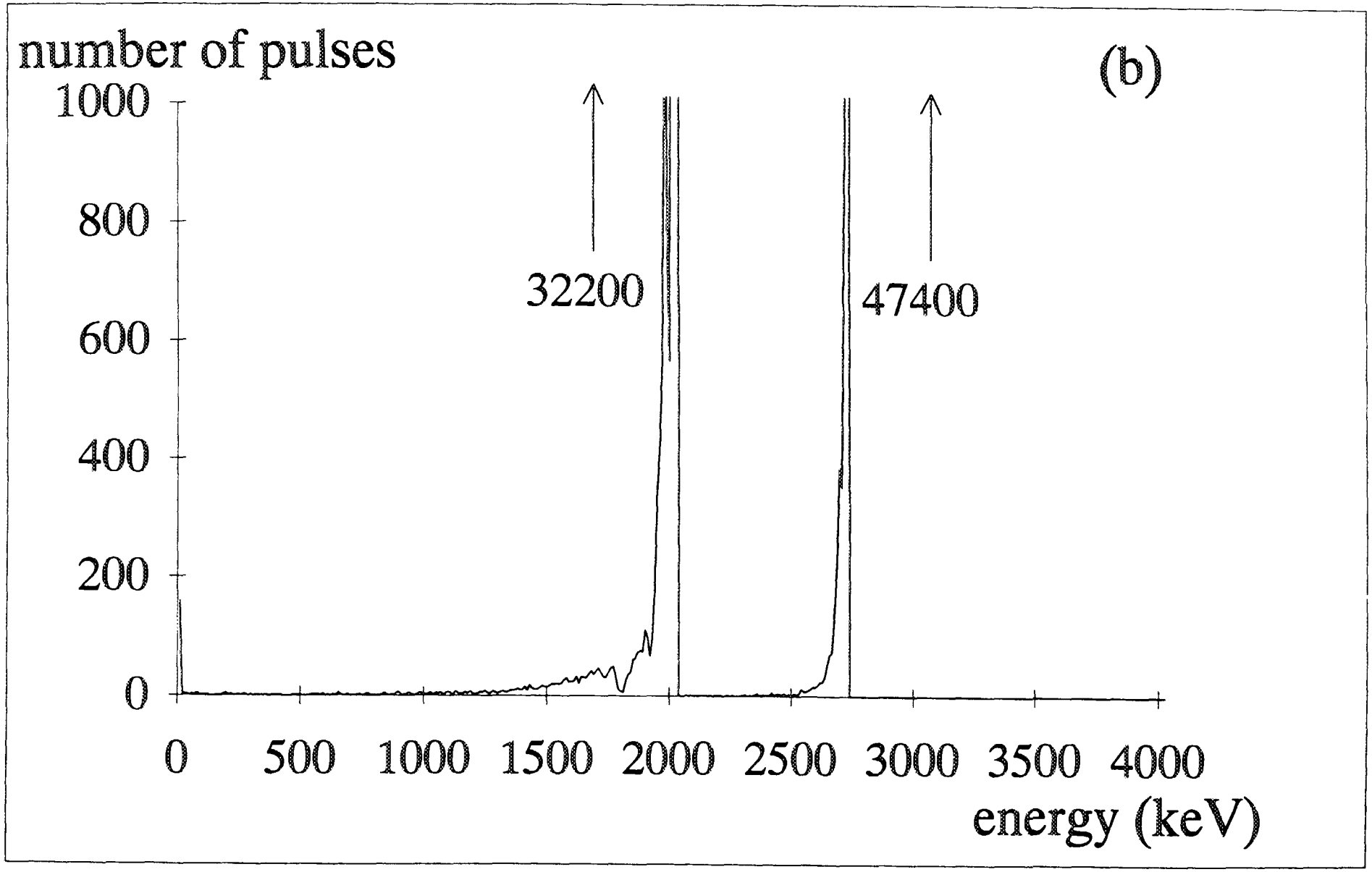
number of pulses
(b)
1000
800
600
400
200
0
32200
47400
0
500
1000
1500
2000
2500
3000
3500
4000
energy (keV)

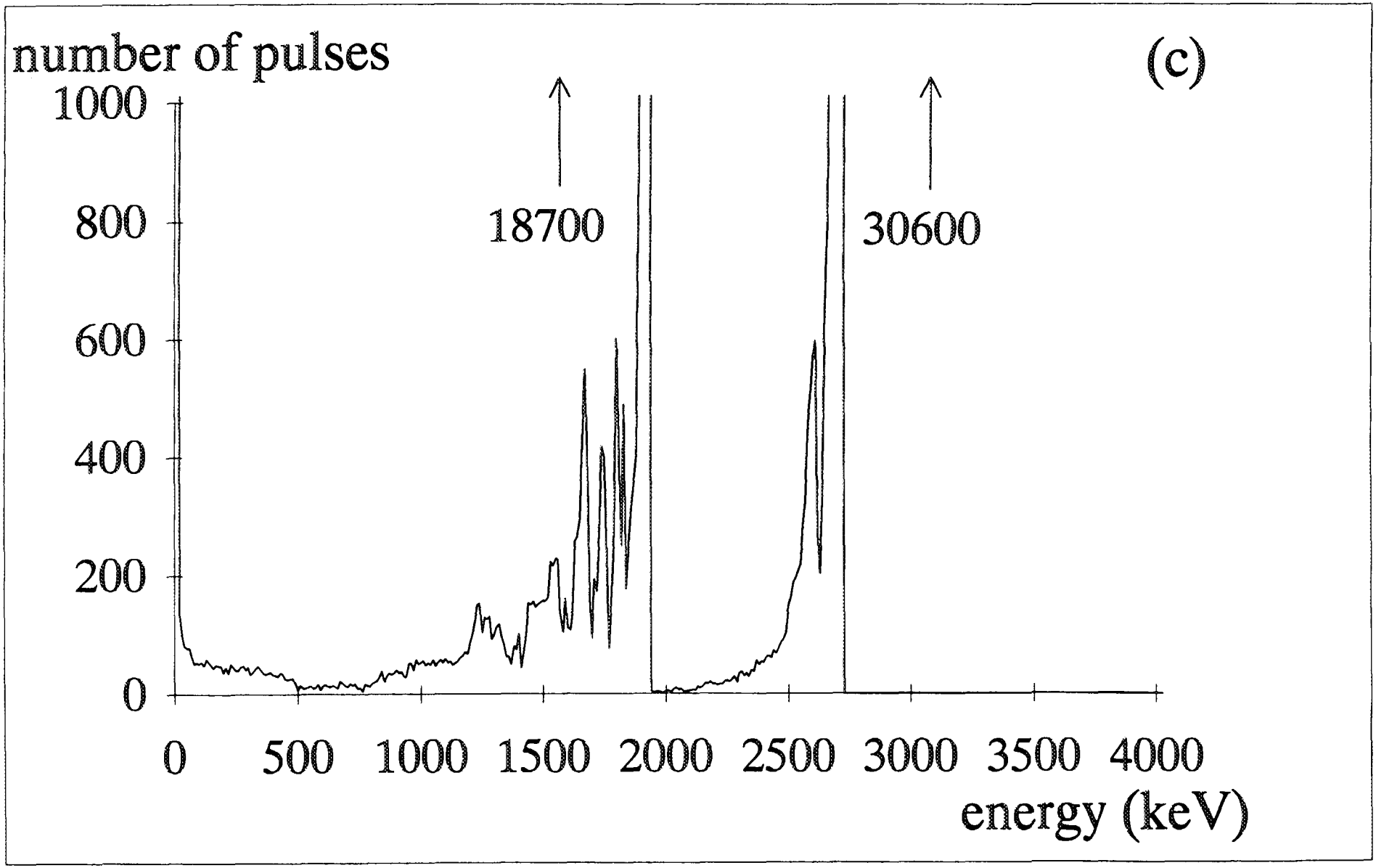
number of pulses
(c)
1000
800
600
400
200
0
18700
30600
0
500
1000
1500
2000
2500
3000
3500
4000
energy (keV)

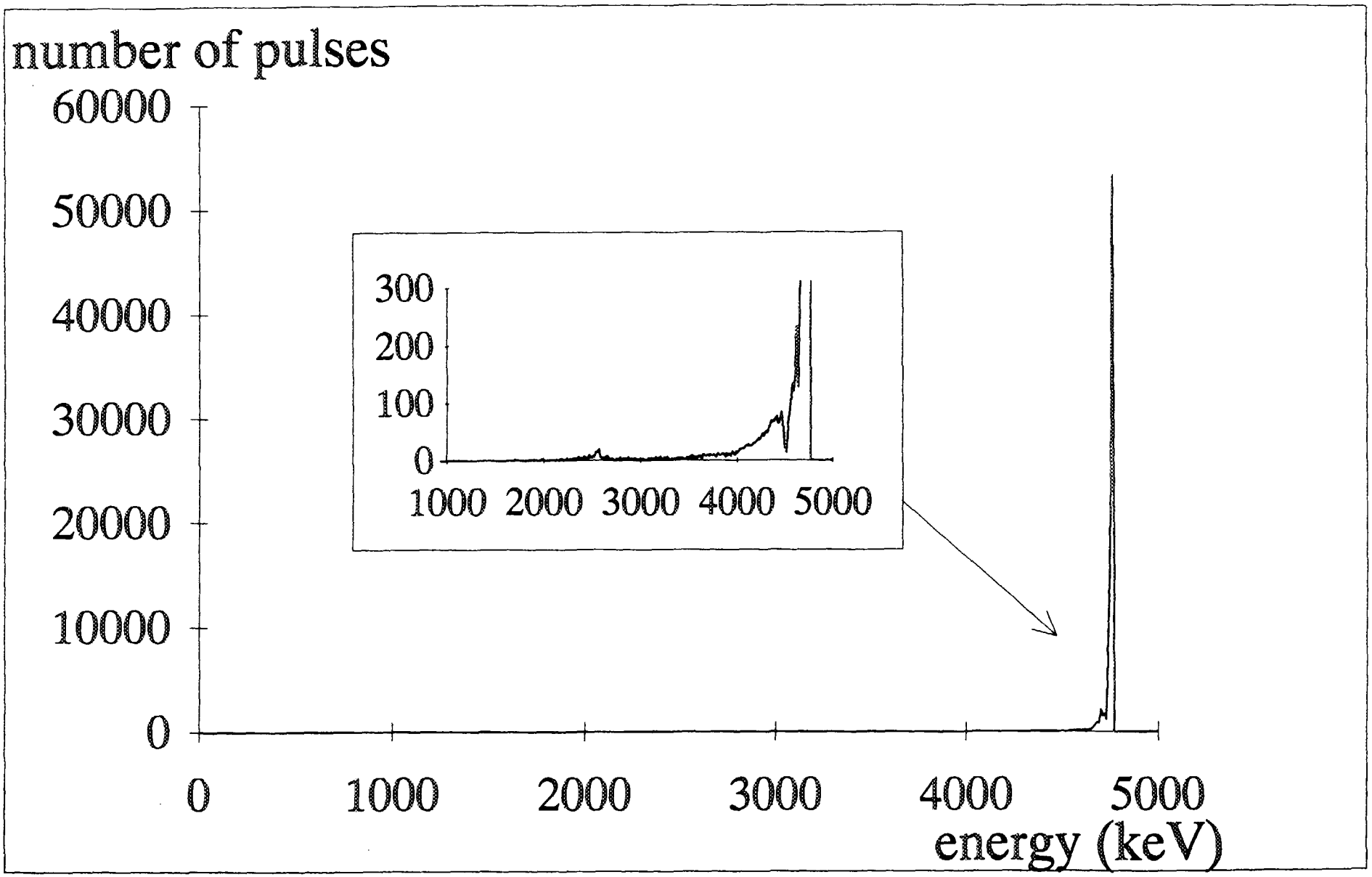
number of pulses
60000
50000
40000
30000
20000
10000
0
0
1000
2000
3000
4000
5000
energy (keV)
300
200
100
0
1000
2000
3000
4000
5000

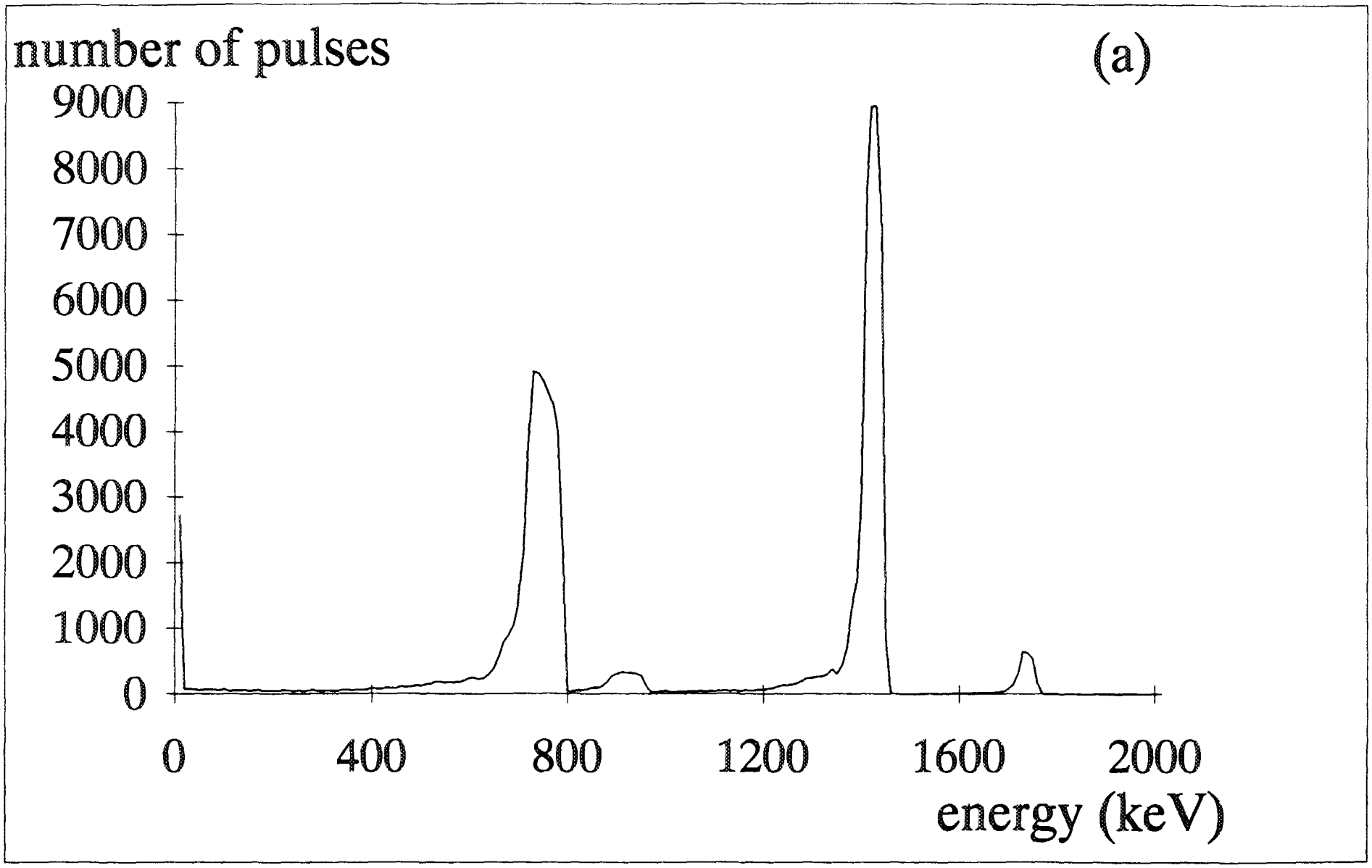
number of pulses
(a)
9000
8000
7000
6000
5000
4000
3000
2000
1000
0
0
400
800
1200
1600
2000
energy (keV)

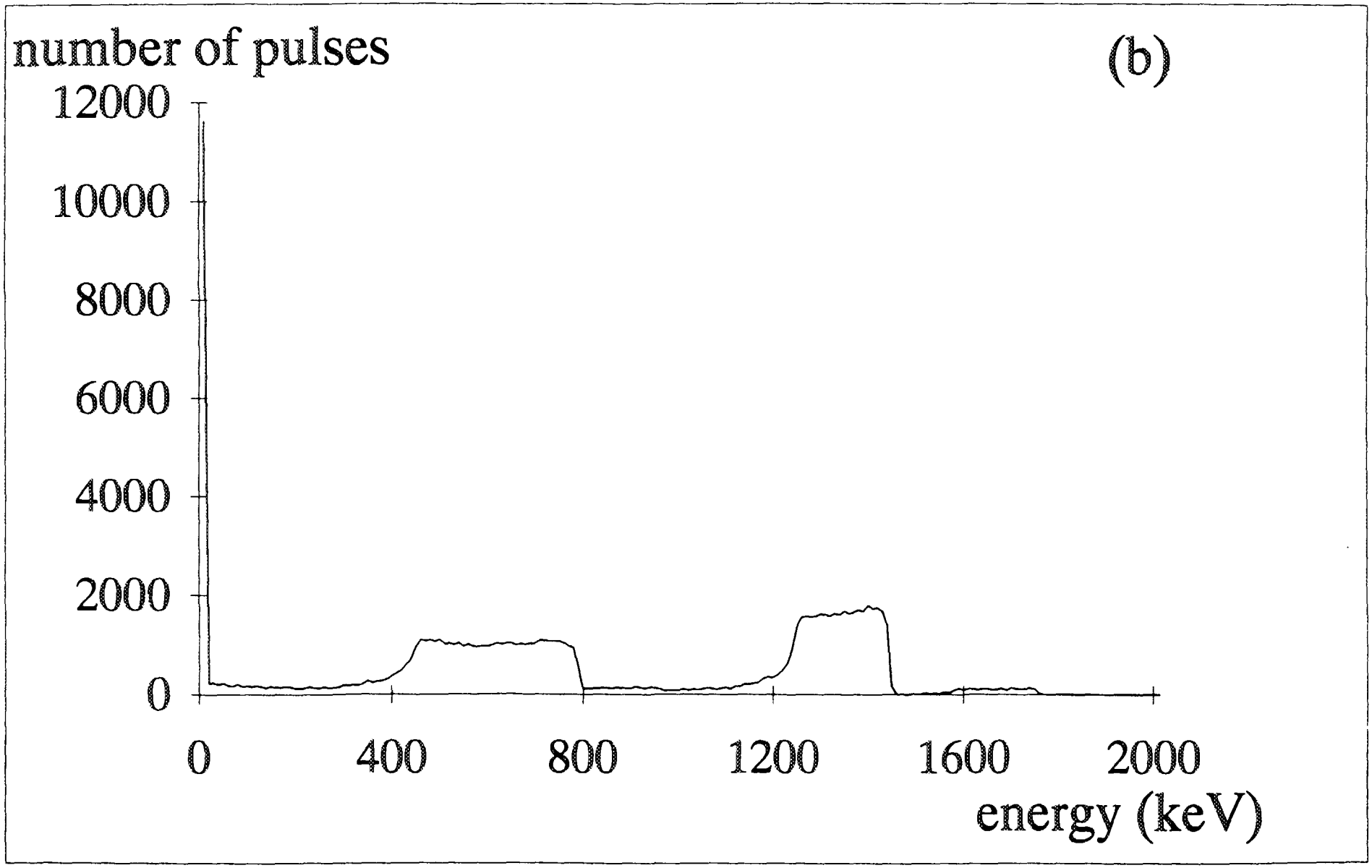
number of pulses
(b)
12000
10000
8000
6000
4000
2000
0
0
400
800
1200
1600
2000
energy (keV)

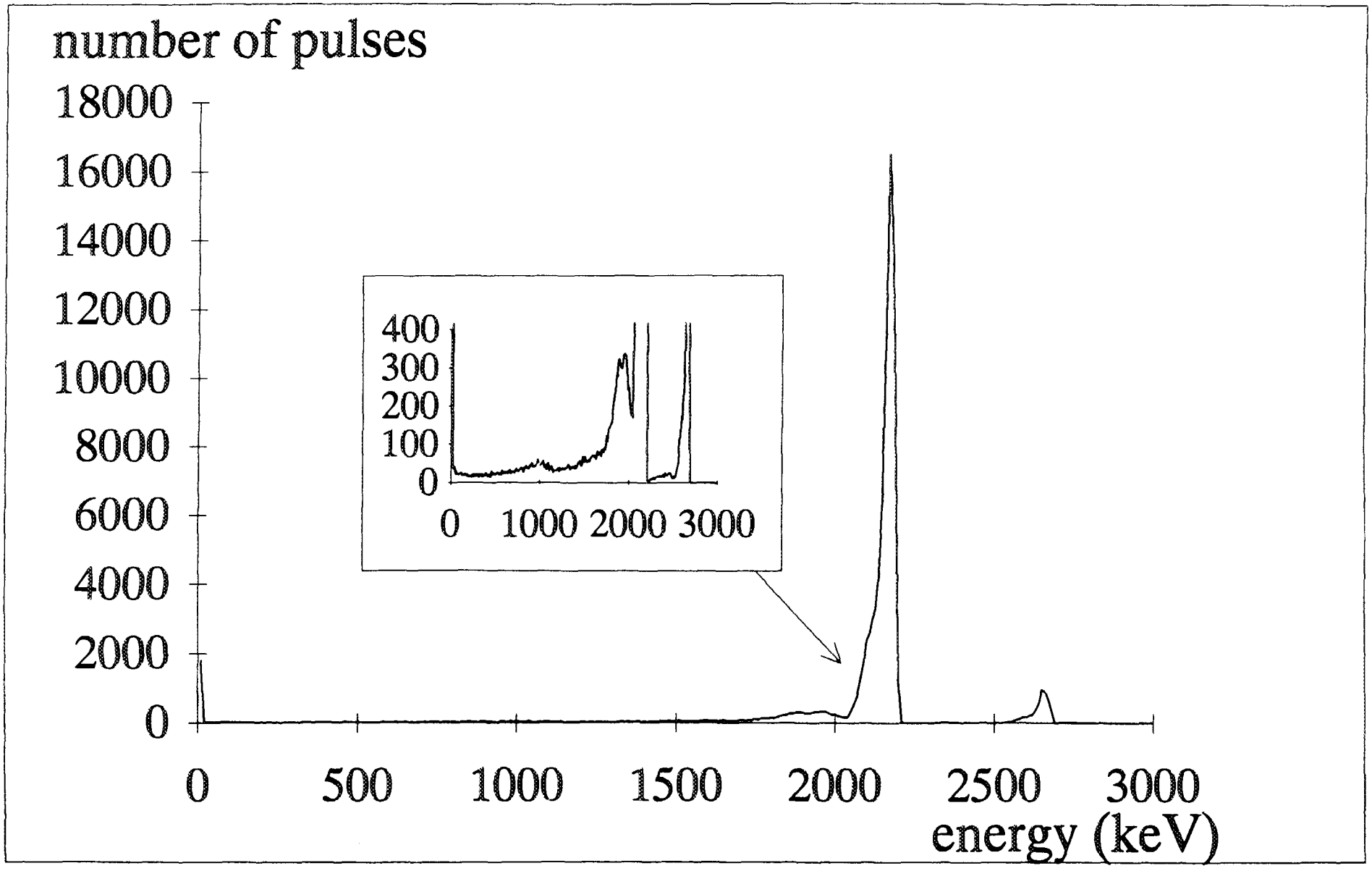
number of pulses
18000
16000
14000
12000
10000
8000
6000
4000
2000
0
0
500
1000
1500
2000
2500
3000
energy (keV)
400
300
200
100
0
0
1000
2000
3000

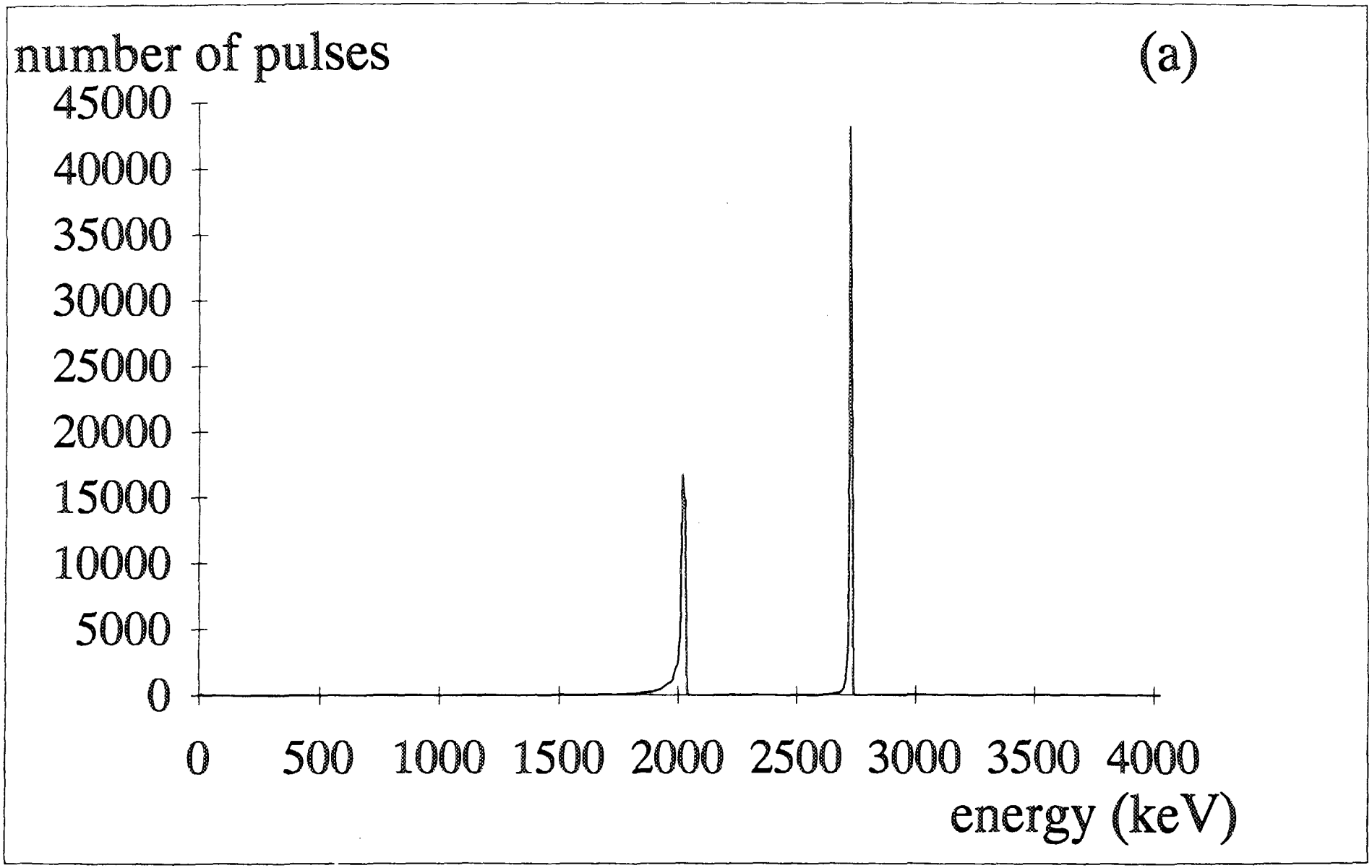
number of pulses
(a)
45000
40000
35000
30000
25000
20000
15000
10000
5000
0
0
500
1000
1500
2000
2500
3000
3500
4000
energy (keV)

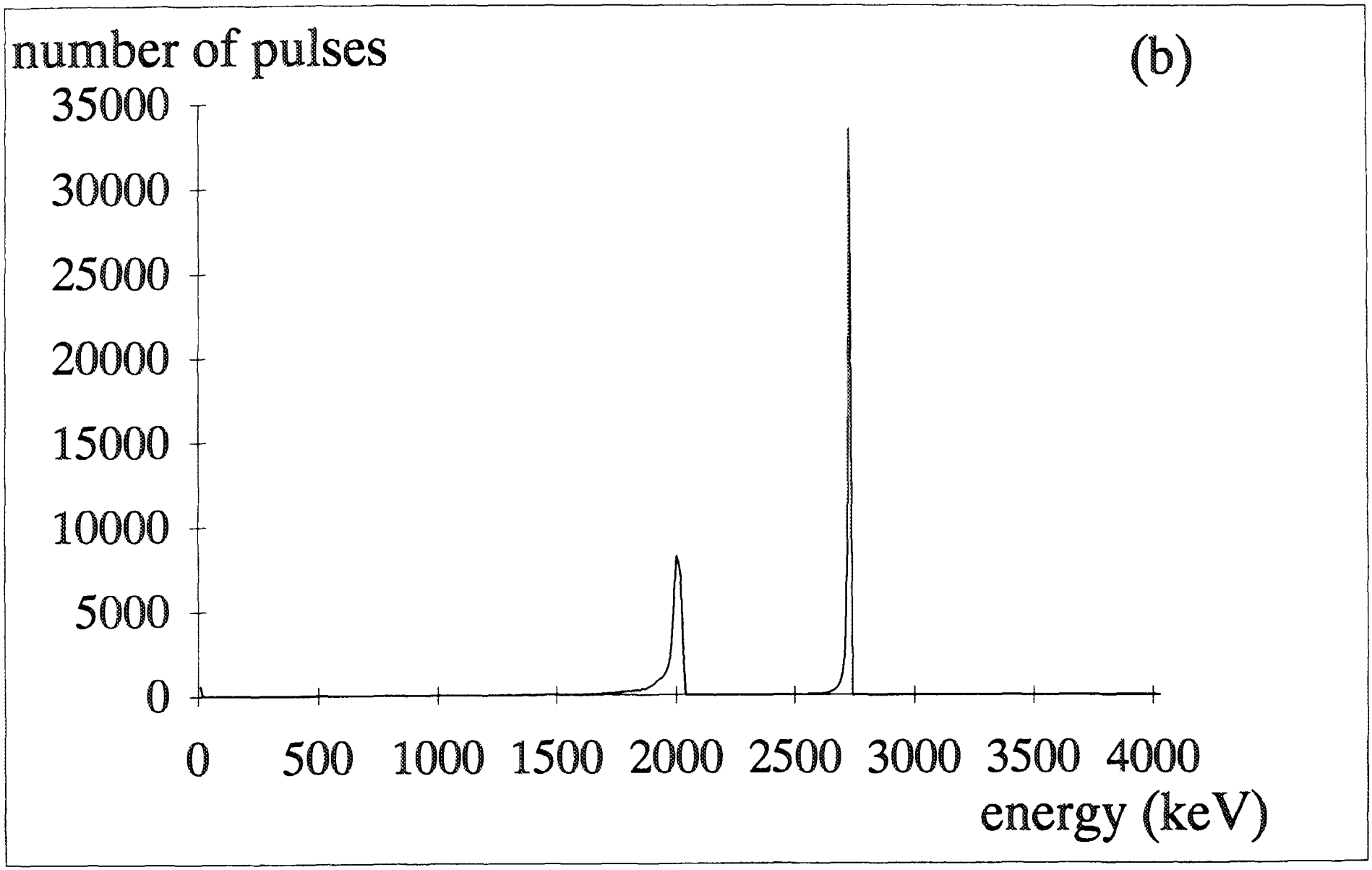
number of pulses
(b)
35000
30000
25000
20000
15000
10000
5000
0
0
500
1000
1500
2000
2500
3000
3500
4000
energy (keV)

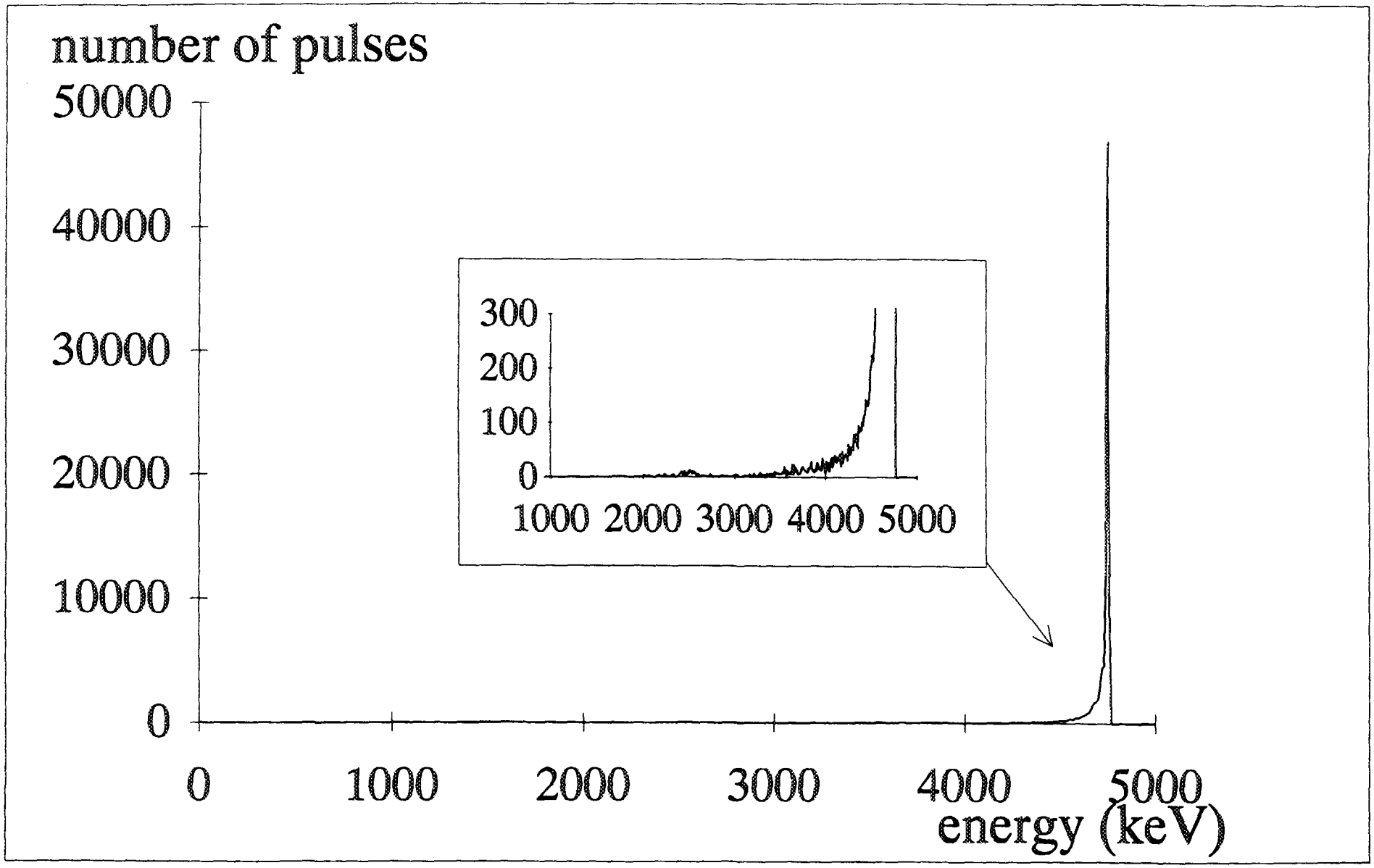
number of pulses
50000
40000
30000
20000
10000
0
0
1000
2000
3000
4000
5000
energy (keV)
300
200
100
0
1000 2000 3000 4000 5000

Emax	0.90 * Emax	0.95 * Emax
2.24 MeV	5 %	10.8 %
2.72 MeV	1.9 %	6.5 %
4.76 MeV	1.7 %	3.1 %

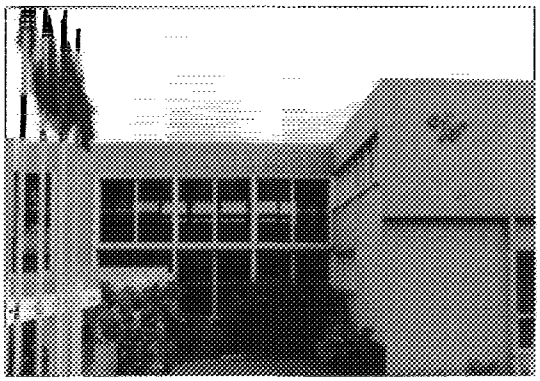

Le LAAS (Laboratoire d'Analyse et d'Architecture des Systèmes) est un laboratoire propre du Centre National de la Recherche Scientifique (CNRS), associé à l'Université Paul Sabatier (UPS), l'Institut National des Sciences Appliquées (INSA) et à l'Institut National Polytechnique de Toulouse (INPT).
Laboratoire du Département des Sciences pour l'Ingénieur (SPI) du CNRS, le LAAS mène ses activités dans cinq grands domaines : AUTOMATIQUE, INFORMATIQUE, MICROELECTRONIQUE, PRODUCTIQUE, ROBOTIQUE.

The LAAS (Laboratory of Analysis and Architecture of Systems) belongs specifically to the CNRS (National Centre for Scientific Research) associated with Paul Sabatier University (UPS), the National Institute of Applied Sciences (INSA) and the National Polytechnic Institute of Toulouse (INPT).
As a laboratory belonging to the Department of Sciences for the Engineer (SPI) of CNRS, the LAAS carries out its activities in five major areas : AUTOMATIC CONTROL, COMPUTER SCIENCE, MICROELECTRONICS, MANUFACTURING SYSTEMS, ROBOTICS.

LAAS-CNRS
7, avenue du colonel-Roche - 31077 TOULOUSE CEDEX
Tél. : (33) 61 33 62 76 - Téléfax : (33) 61 55 35 77
Email : doc@laas.fr